




Cite this: *RSC Adv.*, 2018, 8, 40934

Green synthesis of PbCrO_4 nanostructures using gum of ferula assa-foetida for enhancement of visible-light photocatalytic activity

Rahele Zhiani,^{ab} Ali Es-haghi,^c Seyed Mohsen Sadeghzadeh ^{*ab} and Farzaneh Shamsa^{ab}

Photocatalytic selective oxidation has attracted considerable attention as an environmentally friendly strategy for organic transformations. Some methods have been reported for the photocatalytic oxidation of sulfides into sulfoxides in recent years. However, the practical application of these processes is undermined by several challenges, such as low selectivity, sluggish reaction rates, requirement of UV-light irradiation, use of additives, and instability of the photocatalyst. Pure monoclinic lead chromate nanoparticles were prepared *via* a new simple way as Pb and Cr sources. PbCrO_4 NPs were synthesized *via* a green method in the presence of gum of ferula assa-foetida from $\text{Pb}(\text{NO}_3)_2$ and CrCl_3 as lead and chromium resources, respectively. The structural analysis of the samples confirmed the formation of PbCrO_4 nanostructures in the range of 30 ± 5 nm. The PbCrO_4 nanocatalyst was thoroughly characterized by powder X-ray diffraction (XRD), scanning electron microscopy (SEM), transmission electron microscopy (TEM), and energy dispersive X-ray spectroscopy (EDX) study. Considering the large ionic internal character and high mechanical and thermal stability as well as long-term colloidal stability, this system can be considered as a perfect nanocatalyst by using the host–guest approach. A green and ecofriendly method for oxidation of sulfides to sulfones in the presence of O_2 as an oxidant was examined for the synthesised PbCrO_4 NPs. The easy and applied reusability of the catalyst was observed after the completion of the reaction under visible-light irradiation.

Received 18th August 2018
Accepted 12th November 2018

DOI: 10.1039/c8ra06910g

rsc.li/rsc-advances

Introduction

The oxidation reaction is one of the most vital protocols for changing raw materials into products.^{1–4} Oxidation reactions have some desired features of a ‘green’ procedure in terms of reduced waste production and play key roles in the industry.^{5–9} There are many methods for conventional oxidants for oxidation of sulfide.^{10–19} O_2 is clean, inexpensive, easily accessible and eco-friendly as its side product is only water. The over-oxidation of sulfides resulting in sulfone formation is a common problem. In this regard, intense efforts have been assigned to the expansion of oxidation reactions using green methods and recyclable catalysts that co-produce safe waste.^{20,21} Photocatalytic developments, which use visible light as a great and easily accessible source of energy for catalytic reactions, have been considered to be significant for a sustainable future.^{22,23}

There are some reports on the use of molecular oxygen for the photocatalytic oxidation of sulfides into sulfoxides. Chen

et al. reported photocatalytic systems that exhibited aerobic oxidation of sulfides into sulfoxides by using titanium(IV) oxide as the catalyst.^{24–26} These methods used methanol as the solvent, and it was also oxidized to formaldehyde. Also, Li *et al.* conducted photocatalytic oxidation of sulfides on Pt/BiVO_4 in water under visible-light illumination.²⁷

In the past decades, inorganic nanomaterials have attracted significant interest because of their exclusive properties such as optical, electronic and magnetic properties and potential applications in nanodevices.^{28–32} There are four types of reported oxides in Pb–Cr–O ternary system: PbCrO_4 , Pb_2CrO_5 , Pb_5CrO_8 and $\text{Pb}_{11}\text{CrO}_{16}$. Three compounds with $\text{Pb}(\text{Pb})_n\text{CrO}_4$ ($n = 0, 1, 4$) composition are known to have optoelectronic properties. PbCrO_4 crystallizes in two structures such as stable monoclinic and unstable orthorhombic.³³ PbCrO_4 is an important solid material that is applied as a photosensitizer; it has a stable monoclinic structure and is yellow pigment because of its thermal stability and electrical properties.³⁴ Lead chromate is a significant photocatalyst material. It has been widely applied in decorative and protective systems and mass coloration of fibers, plastics and elastomers.^{35,36} Also, lead chromate has been applied as a host material for humidity-sensing resistors, photosensitizers and other devices.³⁷

^aNew Materials Technology and Processing Research Center, Department of Chemistry, Neyshabur Branch, Islamic Azad University, Neyshabur, Iran

^bYoung Researchers and Elite Club, Neyshabur Branch, Islamic Azad University, Neyshabur, Iran. E-mail: seyedmohsen_sadeghzadeh@yahoo.com

^cDepartment of Biology, Mashhad Branch, Islamic Azad University, Mashhad, Iran



Given our continued interest in nanocatalysis and catalyst development for organic reactions,^{38–40} we offer a new, low-temperature and facile route to synthesize nanostructured PbCrO_4 utilizing gum of ferula assa-foetida. To the best of our knowledge, it is our first effort to exploit gum of ferula assa-foetida as a novel and renewable catalyst to produce nanostructured PbCrO_4 . The fuel exploited for the fabrication of the nanostructured PbCrO_4 in this research is environmentally friendly and non-toxic. Gum of ferula assa-foetida is rich in ferulic acid as well as disulfite that can play the role of reductant; also, it may be responsible for control over shape and size due to the formation of favorable steric hindrance effect in the synthesis process. The reported method can be easily applied for large-scale production of nanostructured PbCrO_4 . Therefore, herein, we have used the advantages of the properties of PbCrO_4 NPs for the photocatalytic oxidation of sulfide under visible-light irradiation.

Experimental

General procedure for the preparation of PbCrO_4 NPs

Here, 0.5 g of lead nitrate and 1.21 g of chromium chloride were dissolved in distilled water. Then, 2 mmol of citric acid was added to the mixed solution and the pH of the above solution was adjusted to 9 by adding tetraethylenepentamine (TEPA) drop-wise; in the next step, 2 mmol of ethylene glycol as the esterification agent was added to the resultant solution. Increasing temperature and evaporation of the gel-like solution led to the preparation of a porous solid mass. One g of gum of ferula assa-foetida was mixed with prepared powders and calcined at 700 °C for 3 h.

General procedure for the oxidation of sulfide

Here, 0.1 mg of PbCrO_4 NPs, 3 mmol of thioanisole and 0.1 mmol of triethylamine were added to 5 mL of CH_3OH . After the reaction mixture was stirred for 30 min in dark to reach the adsorption equilibrium, O_2 was purged into the vessel to raise the initial pressure to 0.1 MPa. The reaction mixture was magnetically stirred and illuminated with $\lambda > 400$ nm visible light irradiation at room temperature. At the end of reaction, the PbCrO_4 photocatalyst particles were separated from the reaction mixture by filtration and the products were quantitatively analyzed by gas chromatography (GC) equipped with a flame ionization detector (FID) using chlorobenzene as the internal standard.

Compound 2a. Yellow oil, ^1H NMR; δ , ppm: 7.68–7.66 (m, 2H), 7.51–7.40 (m, 3H), 2.67 (s, 3H); ^{13}C NMR; δ , ppm: 145.6, 131.0, 129.3, 123.4, 44.1.

Compound 2b. Yellow oil, ^1H NMR; δ , ppm: 7.48 (d, $J = 8.2$ Hz, 2H), 7.30 (d, $J = 8.2$ Hz, 2H), 2.67 (s, 3H), 2.38 (s, 3H); ^{13}C NMR; δ , ppm: 142.5, 141.1, 130.0, 123.5, 44.1, 21.4.

Compound 2c. Yellow oil, ^1H NMR; δ , ppm: 7.55 (d, $J = 8.7$ Hz, 2H), 7.00 (d, $J = 8.7$ Hz, 2H), 3.76 (s, 3H), 2.65 (s, 3H); ^{13}C NMR; δ , ppm: 161.9, 136.6, 125.2, 114.1, 55.4, 43.8.

Compound 2d. White solid, mp 154–157 °C. ^1H NMR; δ , ppm: 8.34 (d, $J = 8.9$ Hz, 2H), 7.88 (d, $J = 8.9$ Hz, 2H), 2.81 (s, 3H); ^{13}C NMR; δ , ppm: 153.1, 149.3, 124.9, 124.3, 44.1.

Compound 2e. Yellow oil, ^1H NMR; δ , ppm: 7.61 (d, $J = 8.6$ Hz, 2H), 7.50 (d, $J = 8.6$ Hz, 2H), 2.68 (s, 3H); ^{13}C NMR; δ , ppm: 144.4, 137.3, 129.4, 125.0, 43.9.

Compound 2f. Yellow oil, ^1H NMR; δ , ppm: 7.65 (d, $J = 8.4$ Hz, 2H), 7.48 (d, $J = 8.4$ Hz, 2H), 2.70 (s, 3H); ^{13}C NMR; δ , ppm: 145.0, 132.8, 125.3, 124.9, 43.8.

Results and discussion

Crystallite size and respective phase composition of the samples were evaluated by XRD. The crystalline structures of the as-synthesized PbCrO_4 NPs were detected by XRD analysis. Fig. 1 shows the XRD pattern of PbCrO_4 NPs synthesized with $\text{Pb}(\text{NO}_3)_2$ and CrCl_3 . The presence of peaks in the XRD pattern of PbCrO_4 is consistent with the monoclinic structure, which is in agreement with JCPDS standard cards no. 08-0210. PbCrO_4 belongs to the space group $P2_1/n$ and could be identified in some cases by the (011), (120), and (200) peaks, of which the (011) is most distinct from those of other phases. Also, (120) is the most intense line for PbCrO_4 . To prove the correct preparation of PbCrO_4 , EDX pattern was obtained for the sample (Fig. 2). As seen in the spectrum, the sample is composed of Cr, Pb, and O. SEM was used to study the size and morphology of PbCrO_4 . The SEM image of PbCrO_4 showed that the prepared catalyst is nanometer quasi-spherical with an average diameter of 30 ± 5 nm (Fig. 3a). Also, the TEM image of PbCrO_4 is presented in Fig. 3b. It clearly shows well dispersion of the prepared catalyst and several larger structures, which can be ascribed to the aggregation/coalescence of each nanoparticle. Table 1 shows the values of BET surface area, pore size, and pore volume for PbCrO_4 . As for PbCrO_4 , the BET surface area, total pore volume, and pore diameter (nm) are obtained as $719 \text{ m}^2 \text{ g}^{-1}$, $2.73 \text{ cm}^3 \text{ g}^{-1}$, and 24.82 nm, respectively.

Fig. 4 shows the effect of solvent on the catalytic function. The reaction did not proceed in THF or in solvent-free condition and showed low conversion in ethanol and water. Acetonitrile was the best solvent for photocatalytic reactions in certain reports,^{41,42} and it also produced a high conversion of 83.9%.

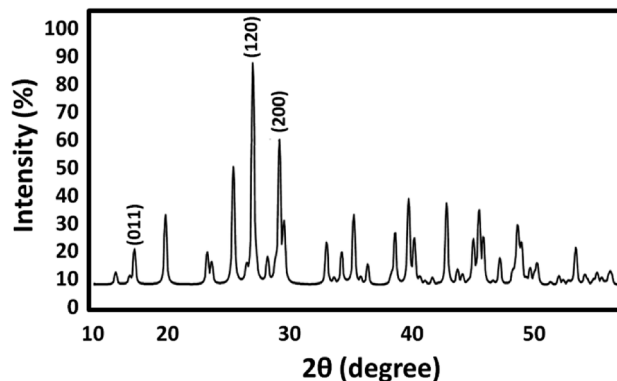


Fig. 1 XRD analysis of PbCrO_4 NPs.

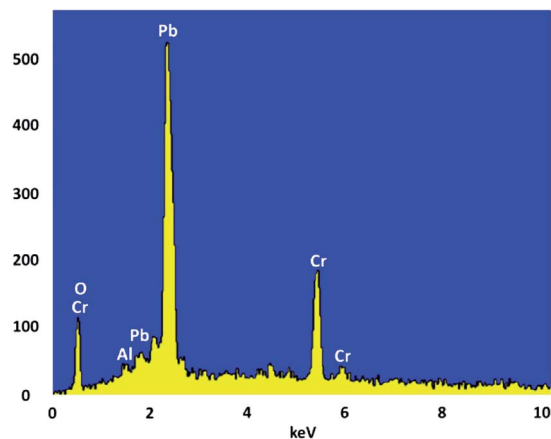


Fig. 2 The EDX spectra of PbCrO₄ NPs.

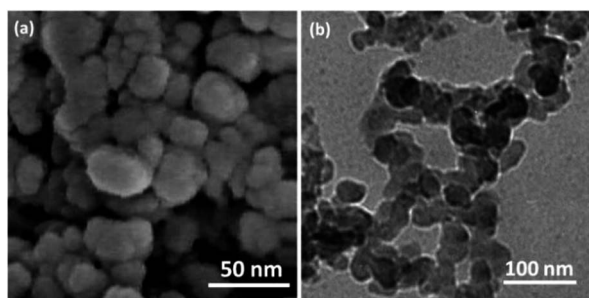


Fig. 3 (a) SEM images of PbCrO₄ NPs; (b) TEM images of PbCrO₄ NPs.

Table 1 Structural parameters of PbCrO₄ NP materials determined from nitrogen sorption experiments

S_{BET} ($\text{m}^2 \text{g}^{-1}$)	V_a ($\text{cm}^3 \text{g}^{-1}$)	Pore diameter (nm)
719	2.73	24.82

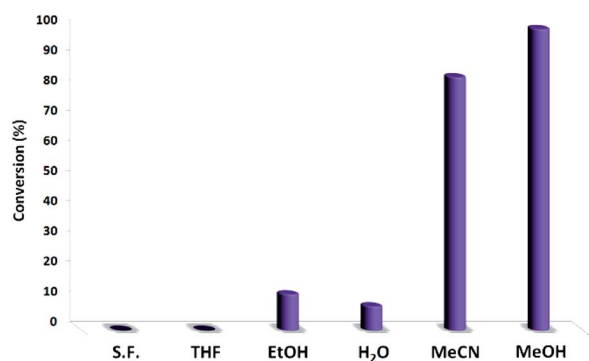


Fig. 4 Photocatalytic oxidation of sulfides in different solvents.

Methanol resulted in 99.9% conversion. Interestingly, the solvent exhibited a great effect on the photocatalytic activity of PbCrO₄ NPs towards the oxidation of thioanisole. Thus, methanol was selected as a safe solvent.

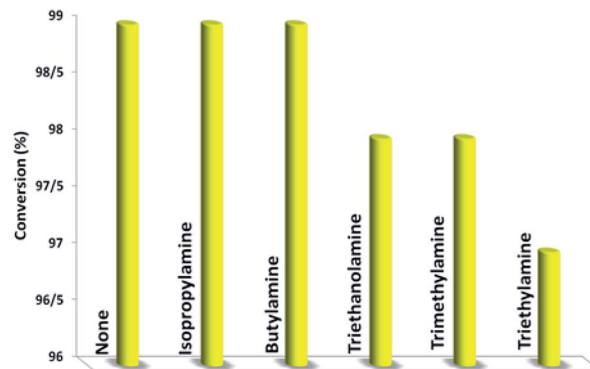


Fig. 5 The influence of amine on the selective aerobic oxidation of thioanisole under visible-light irradiation.

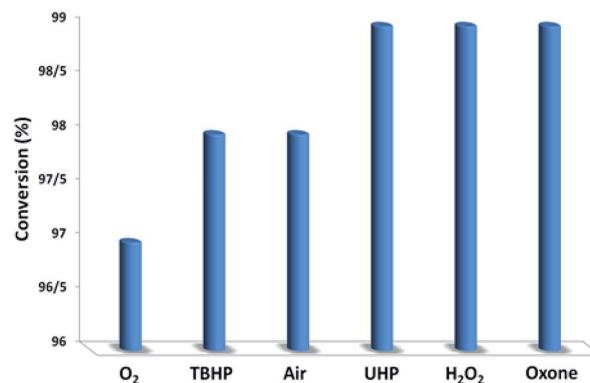


Fig. 6 The screening of the oxidant nature.

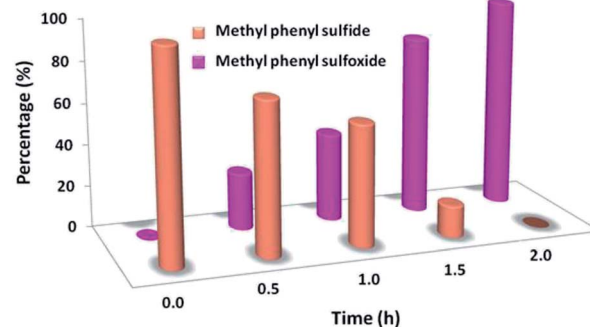


Fig. 7 Time course of the product distribution for the photocatalytic oxidation of methyl phenyl sulfide into methyl phenyl sulfoxide.

In the next step, we conducted aerobic sulfide oxidation with a variety of amines, which could be easily separated from the sulfoxide product (Fig. 5). The conversion of thioanisole without amine was very low under visible-light irradiation. Interestingly, with the introduction of amine into the reaction system, the progression of the reaction was significantly boosted. Primary amines can initiate the oxidation, and a decrease in the amount of amine leads to a decrease in the conversion of the product. As expected, the tertiary amines TMA and TEA remained stable

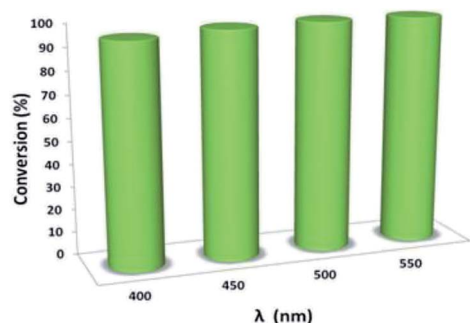


Fig. 8 Control experiment for the synergistic photocatalytic oxidation of thioanisole.

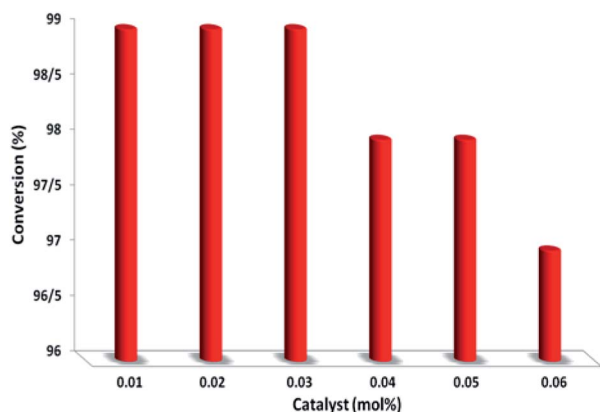


Fig. 9 The effect of catalyst amount.

during the oxidation process, ensuring higher conversions of thioanisole. Based on the data in Fig. 6, common oxidants such as H_2O_2 , TBHP, UHP and oxone were weaker oxidants than O_2 for this transformation. During the reaction process, the concentration of methyl phenyl sulfide gradually decreased, whereas the concentration of methyl phenyl sulfoxide gradually increased (Fig. 7). No intermediates or other by-products were observed during the reaction process. After light irradiation for 2 h, methyl phenyl sulfide was quantitatively converted into the target product of methyl phenyl sulfoxide.

Moreover, the reaction shows light-wavelength-dependent behavior. Thus, a wide range of visible-light spectra can be used for this reaction, representing a giant step forward compared to the results obtained in previous reports, where only visible light of approximately 400 nm could be used (Fig. 8).

Table 3 Substrate scope of the oxidation of sulfides into sulfoxides

Entry	Substrate	Product	Conversion [%]
1			99.9
2			99.9
3			99.9
4			87.2
5			83.9
6			86.1

To further prove the catalytic nature of PbCrO_4 , we varied the amount of PbCrO_4 used in the reaction to study its effect on the selective aerobic oxidation of thioanisole under visible-light irradiation; more details and results are summarized in Fig. 9. We discovered that decreasing the amount of PbCrO_4 led to a drop in conversion to some extent in comparison with the starting result. Increasing PbCrO_4 did not lead to an apparent increase in conversion. These combined results prove that PbCrO_4 truly acts as a catalyst for the photoredox process.

In comparison to previously reported methods, our method is milder, greener from viewpoint of oxidant, support, and

Table 2 An overview of some methods for oxidation of thioanisole

Entry	Catalyst	Solvent	Oxidant	T (°C)	t (h)	Yield (%)
1	Na_2WO_4	H_2O	H_2O_2	50	1.0	97 (ref. 43)
2	Ti^{4+}	CCl_4	TBHP	25	9.0	28 (ref. 44)
3	—	MeOH	Oxone	0	0.03	84 (ref. 45)
4	$[\text{WO}_4][\text{SiO}_2/\text{PrNH}_3]_2$	DCM/MeOH	H_2O_2	25	0.5	82 (ref. 46)
5	$\text{VO}(\text{salen})$	DCM	CHP	-20	720.0	79 (ref. 47)
6	PbCrO_4	MeOH	O_2	25	2.0	99

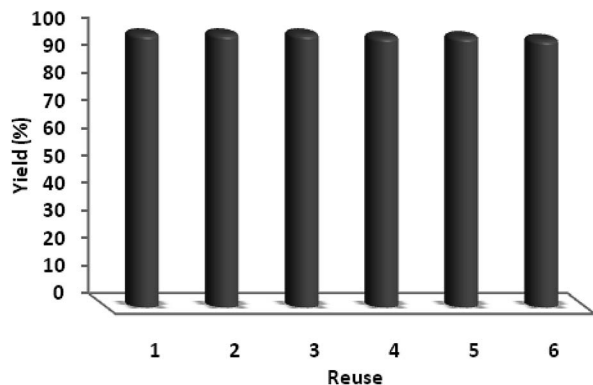
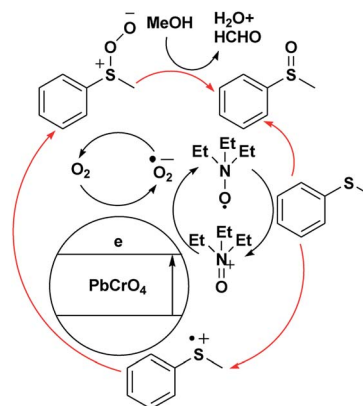


Fig. 10 The reusability of catalysts for the oxidation of thioanisole.



Scheme 1 Possible mechanism for the visible-light-induced oxidation of sulfides with O_2 .

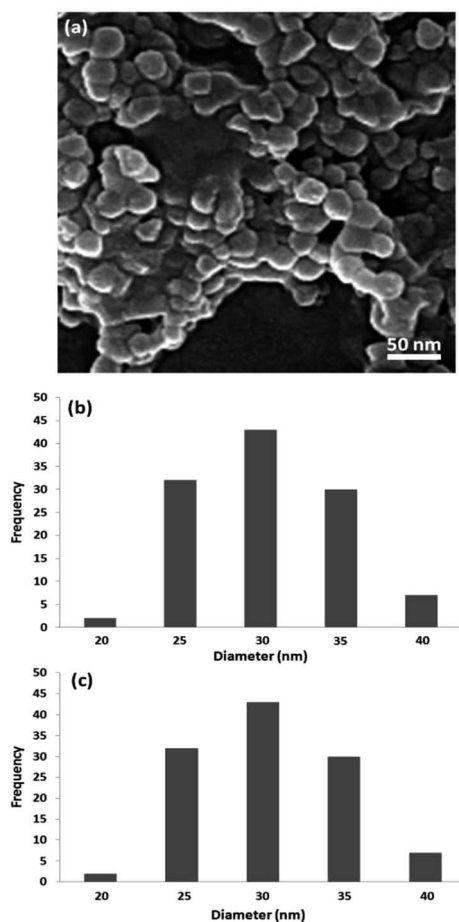


Fig. 11 TEM images of $PbCrO_4$ nano-catalysts after reaction (a). Particle size distribution before reaction (b) and after reaction (c).

metal; it is also cost-effective with higher conversion and selectivity towards production of sulfoxide. This comparison clearly exhibits that our proposed catalyst is excellent (Table 2).

After the formulation of tentative reaction mechanism, we finally seek to establish the scope of the substrates for this visible-light photoredox catalysis, which is important for demonstrating the generality of this reaction scheme. The

reaction results are summarized in Table 3. The sulfides were successfully oxidized into the corresponding sulfoxides with good to excellent yields. The electronic properties of the substituents in the aryl sulfides played an important role in the substrate activity. Generally, the substrates with electron-donating groups demonstrate higher activity than the substrates with electron-withdrawing groups; the latter require longer reaction times to give high yields of the corresponding sulfoxides. The substrates with electron-donating groups more easily donate electrons to sulfur atoms than the substrates with electron-withdrawing groups, which can be beneficial for the oxidation reactions.

One of the most important merits of heterogeneous catalysts is that they can be recycled and reused. Thus, the recyclability of the $PbCrO_4$ catalyst was investigated for the oxidation of thioanisole. After the first catalytic run, the catalyst was separated by centrifugation, leached and washed with water and methanol, and dried at $80^\circ C$ under vacuum. The used $PbCrO_4$ catalyst was subjected to a next run under the same conditions. As shown in Fig. 10, the $PbCrO_4$ catalyst demonstrated excellent recyclability. It was recycled six consecutive times with almost unaltered catalytic activity.

The catalytic activity of nano- $PbCrO_4$ depends on the size of the particles, and we observed that $PbCrO_4$ nanoparticles with sizes are effective in catalyzing reactions. However, these nanoparticles generally lose their activity slowly during every reaction cycle. This loss in activity is observed because the nanoparticles grow in size through the Ostwald ripening process, in which small nanoparticles merge together to form large nanoparticles. In the case of the $PbCrO_4$ catalyst system, we observed no appreciable Ostwald ripening, and the particle size and distribution remained the same even after the reaction, which in turn maintained the catalytic activity. Therefore, even after several reaction cycles, the size and distribution of $PbCrO_4$ nanoparticles remain nearly the same (Fig. 11) and thus, the system maintains nearly the same catalytic activity.

The tentative mechanism of visible-light photoredox catalysis by $PbCrO_4$ with triethylamine as a redox mediator is rationalized in Scheme 1. $PbCrO_4$ can absorb a wide range of visible

light. Next, the electron travels through the conduction band of PbCrO_4 to react with O_2 , thereby forming $\text{O}_2^{\cdot-}$. The S-centered free-radical cation prefers to react with $\text{O}_2^{\cdot-}$ formed at the conduction band of PbCrO_4 , allowing the evolution of sulfide peroxide. In the protic solvent CH_3OH , the final methyl phenyl sulfoxide is formed, accompanied by the side products of HCHO and H_2O . At this stage, this proposed mechanism lacks direct evidence (Scheme 1).

Conclusions

In conclusion, PbCrO_4 nanoparticles were successfully synthesized *via* a green method in the presence of gum of ferula assafoetida as a novel nanocatalyst. SEM, TEM, XRD and EDX have been used to characterize the prepared nanocatalyst. Through the photocatalysis of PbCrO_4 and TEA, the visible-light-induced selective oxidation of sulfide into sulfoxide with O_2 was successfully conducted in CH_3OH . The interaction between PbCrO_4 and TEA gives rise to visible-light activity in the reaction system. This separable solid nanocatalyst can be prepared by a very simple procedure using inexpensive and commercially available precursors, and the catalyst can be reused for six cycles without any loss in its activity as well as composition. Thus, the procedure serves as a valuable alternative in the selective synthesis of sulfoxides.

Conflicts of interest

There are no conflicts to declare.

Notes and references

- 1 Y. C. Ling, G. M. Wang, J. Reddy, C. C. Wang, J. Z. Zhang and Y. Li, *Angew. Chem., Int. Ed.*, 2012, **51**, 4074–4079.
- 2 N. Dimitratos, J. A. Lopez-Sanchez and G. J. Hutchings, *Chem. Sci.*, 2012, **3**, 20–44.
- 3 M. Bordeaux, A. Galarneau and J. Drone, *Angew. Chem.*, 2012, **124**, 10870–10881.
- 4 S. R. Zhang, L. Nguyen, Y. Zhu, S. H. Zhan, C. K. Tsung and F. Tao, *Acc. Chem. Res.*, 2013, **46**, 1731–1739.
- 5 R. Blume, M. Hvecker, S. Zafeiratos, D. Techner, A. KnopGercke, R. Schlgl, L. Gregoratti, A. Barinov and M. Kiskinova, *Nanostructured Catalysts: Selective Oxidations*, The Royal Society of Chemistry, 2011, pp. 248–265.
- 6 J. Piera and J.-E. Bäckvall, *Angew. Chem., Int. Ed.*, 2008, **47**, 3506–3523.
- 7 F. Geilen, B. Engendahl, A. Harwardt, W. Marquardt, J. Klankermayer and W. Leitner, *Angew. Chem.*, 2010, **122**, 5642–5646.
- 8 Z. Guo, B. Liu, Q. Zhang, W. Deng, Y. Wang and Y. Yang, *Chem. Soc. Rev.*, 2014, **43**, 3480–3524.
- 9 T. Matsumoto, M. Ueno, N. Wang and S. Kobayashi, *Chem.–Asian J.*, 2008, **3**, 196–214.
- 10 P. S. Kulkarni and C. A. M. Afonso, *Green Chem.*, 2010, **12**, 1139–1149.
- 11 M. V. Gómez, R. Caballero, E. Vázquez, A. Moreno, A. Hoz and Á. Díaz-Ortiz, *Green Chem.*, 2007, **9**, 331–336.
- 12 B. Karimi, M. Ghoreishi-Nezhad and J. H. Clark, *Org. Lett.*, 2005, **7**, 625–628.
- 13 R. Noyori, M. Aoki and K. Sato, *Chem. Commun.*, 2003, 1977–1986.
- 14 K. Sato, M. Aoki and R. Noyori, *Science*, 1998, **281**, 1646–1647.
- 15 K. Sato, M. Hyodo, M. Aoki, X.-Q. Zheng and R. Noyori, *Tetrahedron*, 2001, **57**, 2469–2476.
- 16 P. Kowalski, K. Mitka, K. Ossowska and Z. Kolarska, *Tetrahedron*, 2005, **61**, 1933–1953.
- 17 K. Kaczorowska, Z. Kolarska, K. Mitka and P. Kowalski, *Tetrahedron*, 2005, **61**, 8315–8327.
- 18 B. M. Choudary, B. Bharathi, C. V. Reddy and M. L. Kantam, *J. Chem. Soc., Perkin Trans. 1*, 2002, 2069–2074.
- 19 K. Jeyakumar, R. D. Chakravarthy and D. K. Chand, *Catal. Commun.*, 2009, **10**, 1948–1951.
- 20 C. M. Gordon, *Appl. Catal., A*, 2001, **222**, 101–117.
- 21 S. Rostamnia, *RSC Adv.*, 2015, **5**, 97044–97065.
- 22 B. Zhou, J. Song, Z. Zhang, Z. Jiang, P. Zhang and B. Han, *Green Chem.*, 2017, **19**, 1075–1081.
- 23 W. Huang, B. C. Ma, H. Lu, R. Li, L. Wang, K. Landfester and K. Zhang, *ACS Catal.*, 2017, **7**, 5438–5442.
- 24 X. Lang, J. Zhao and X. Chen, *Angew. Chem., Int. Ed.*, 2016, **55**, 4697–4700.
- 25 X. Lang, W. Hao, W. R. Leow, S. Li, J. Zhao and X. Chen, *Chem. Sci.*, 2015, **6**, 5000–5005.
- 26 X. Lang, W. R. Leow, J. Zhao and X. Chen, *Chem. Sci.*, 2015, **6**, 1075–1082.
- 27 B. Zhang, J. Li, B. Zhang, R. Chong, R. Li, B. Yuan, S.-M. Lu and C. Li, *J. Catal.*, 2015, **332**, 95–100.
- 28 S. J. Tans, M. H. Devoret, H. Dai, A. Thess, R. E. Smalley, L. J. Geerligs and C. Dekker, *Nature*, 1997, **386**, 474–476.
- 29 J. Wang, M. S. Gudiksen, X. Duan, Y. Cui and C. M. Lieber, *Science*, 2001, **293**, 1455–1457.
- 30 H. Kind, H. Yan, B. Messer, M. Law and P. Yang, *Adv. Mater.*, 2002, **14**, 158–160.
- 31 J. Hu, T. W. Odom and C. M. Lieber, *Acc. Chem. Res.*, 1999, **32**, 435–445.
- 32 X. G. Peng, L. Manna, W. D. Yang, J. Wickham, E. Scher, A. Kadavanich and A. P. Alivisatos, *Nature*, 2000, **404**, 59–61.
- 33 K. S. Knight, *Mineral. Mag.*, 2000, **64**, 291–300.
- 34 S. Vaucher, M. Li and S. Mann, *Angew. Chem., Int. Ed.*, 2000, **39**, 1793–1796.
- 35 X. L. Hu and Y. J. Zhu, *Chem. Lett.*, 2004, **33**, 880–881.
- 36 L. J. H. Erkens, H. Hamers, R. J. M. Hermans, E. Claeys and M. Bijnens, *Surf. Coat. Int., Part B*, 2001, **84**, 169–176.
- 37 K. A. Wishah and M. M. Abdul-Gader, *Appl. Phys. A*, 1998, **66**, 229–234.
- 38 S. M. Sadeghzadeh, *Appl. Organomet. Chem.*, 2016, **30**, 835–842.
- 39 M. A. Nasser and S. M. Sadeghzadeh, *J. Iran. Chem. Soc.*, 2014, **11**, 27–33.
- 40 S. M. Sadeghzadeh, *Microporous Mesoporous Mater.*, 2016, **234**, 310–316.
- 41 Z. Chai, T.-T. Zeng, Q. Li, L.-Q. Lu, W.-J. Xiao and D. Xu, *J. Am. Chem. Soc.*, 2016, **138**, 10128–10131.

- 42 F. Raza, J. H. Park, H.-R. Lee, H.-I. Kim, S.-J. Jeon and J.-H. Kim, *ACS Catal.*, 2016, **6**, 2754–2759.
- 43 K. Sato, M. Hyodo, M. Aoki, X.-Q. Zheng and R. Noyori, *Tetrahedron*, 2001, **57**, 2469–2476.
- 44 N. Komatsu, M. Hashizume, T. Sugita and S. Uemura, *J. Org. Chem.*, 1993, **58**, 4529–4533.
- 45 B. M. Trost and D. P. Curran, *Tetrahedron Lett.*, 1981, **22**, 1287–1290.
- 46 B. Karimi, M. Ghoreishi-Nezhad and J. H. Clark, *Org. Lett.*, 2005, **7**, 625–628.
- 47 K. Nakajima, K. Kojima, M. Kojima and J. Fujita, *Bull. Chem. Soc. Jpn.*, 1990, **63**, 2620–2630.